

Identification of dark axisymmetric plasma modes in partially gated two-dimensional electron gas disk

M.V. Cheremisin

A.F.Ioffe Physical-Technical Institute, St.Petersburg, Russia

(Dated: November 17, 2023)

We investigate the dark axisymmetric plasmon spectrum for partially gated two-dimensional gas of the disk shape. The extension of the central gate spot provides a change in plasmon dispersion from the root to a linear dependence on the wave vector. Intriguingly, the interaction between neighboring modes occurs because of stepwise change in carrier screening across the circumference of the gate. This behavior is unexpected when changing from a fully screened to unscreened two-dimensional gas by increasing the dielectric width under the gate [A.L.Fetter, Phys.Rev.B 33, 5221 (1986)]. Our results provide the accurate identification of axisymmetric plasmon modes recently observed in experiment and, in addition, pave the way for feedback plasmon resonator study.

Plasma oscillations in two-dimensional(2D) electron gas were first predicted in the 60s by F.Stern¹ for ungated and, then analyzed for gated systems². Over the next decade the plasmon assisted infrared absorption³⁻⁶ and emission⁷ has been reported. Since the Stern's pioneering discovery the enormous efforts were done to clarify the plasmon behavior found to be influenced by magnetic field⁸⁻¹⁰, retardation effects¹¹, sample geometry¹²⁻¹⁴ and quality^{15,16}.

A decade ago it was shown¹⁷⁻¹⁹ that the plasma oscillations in two-dimensional systems with arbitrary attached gates and contacts can be elegantly described in terms of classical theory of electrical circuits with distributed parameters. The proposed quasi-static LC approach is extremely powerful for description of plasmon excitations in quasi one-dimensional stripes of 2D gas with periodic grating²⁰. Highly motivated by recent experiments dealt with axisymmetric plasmon excitations observed²¹⁻²³ in partially gated 2D disk we attempt to probe LC approach in this case. Indeed, the axisymmetric modes known^{12,24,25} to have zero angular momentum $l = 0$ and, therefore are called "dark" because of weak coupling with external electromagnetic fields. Arguing that axisymmetric modes are purely radial we will use one-dimensional LC-approach¹⁹ in order to find the plasmon spectra and, then compare theory predictions with recent experimental data. In present study we will disregard the anomalous Goos-Hänchen phase shift^{26,27} of incident and reflected plasma waves at the sharp edge of 2D gas. Then we will confirm the validity of the current use of the quasi-static LCD approach for the analysis of real experimental data.

Let us consider two-dimensional electron system of disk geometry depicted by shaded area in Fig.1, inset. The 2D gas mesa of radius R is grounded peripherally and, moreover, embedded into an homogeneous environment of a dielectric constant ϵ . The cylindrical slab of the height h is covered atop by the gate of radius $r_0 \leq R$. The device is surrounded by air. For clarity, we will assume that the radius R of 2DEG is fixed. In contrast, the slab height h and the gate radius r_0 may vary. Let us first consider the simple case of totally gated 2D gas, i.e when $r_0 = R$ and variable height $0 < h < \infty$ of the slab.

In general, the LC approach¹⁹ is based on hydrodynamic model¹² which includes the Euler equation and the continu-

ity equation for two-dimensional electron gas. Instead of a complete set of Maxwell's equations, taking into account the retardation²⁵, a quasi-static Poisson equation is used to find the in-plane potential of a two-dimensional gas. In what follows we will demonstrate that retardation effects are insignificant for the actual experimental data²¹⁻²³. According to Ref.¹² the set of equations constituent the hydrodynamic model could be linearized with respect to small amplitude of plasma wave excitations. Fortunately, the model can be greatly simplified down to so-called telegrapher's equations¹⁹ for radial components of in-plane potential \tilde{U} and the current \tilde{I} :

$$\frac{\partial \tilde{U}}{\partial r} = -L \frac{\partial \tilde{I}}{\partial t}, \quad (1)$$

$$\frac{\partial \tilde{I}}{\partial r} = -C \frac{\partial \tilde{U}}{\partial t}, \quad (2)$$

$$L(r) = \frac{m^*}{e^2 n} \frac{1}{2\pi r}, \quad C(r) = \frac{(1 + \coth(qh))\epsilon q r}{2}. \quad (3)$$

Here, L , C are the inductance and capacitance per unit length respectively, m^* and n are the effective mass and density of 2D carriers. Then, q is the plasmon wave vector originating from solution of the Poisson equation taking into account the actual dielectric environment.

We now search the solution of Eq.(1,2) separating the temporal and spatial components for potential $\tilde{U} = U(r) \exp(i\omega t)$ and current $\tilde{I} = I(r) \exp(i\omega t)$. Finally, the equation for radial part of the potential $U(r)$ yields:

$$\frac{d^2 U}{d\rho^2} + \frac{1}{\rho} \frac{dU}{d\rho} + U = 0. \quad (4)$$

Here, we introduced the dimensionless radius $\rho = r/\lambda$, where $\lambda = \frac{1}{\omega\sqrt{LC}}$ is the length scale of the problem. The general solution of Eq.(4) is given by the sum of zero order Bessel functions of first(second) kind, namely

$$U(\rho) = A J_0(\rho) + B Y_0(\rho). \quad (5)$$

The arbitrary constants in Eq.(5) can be found by use of a certain boundary conditions. Arguing the potential is finite in the disk center $\rho \rightarrow 0$ we put $B = 0$ to avoid divergent

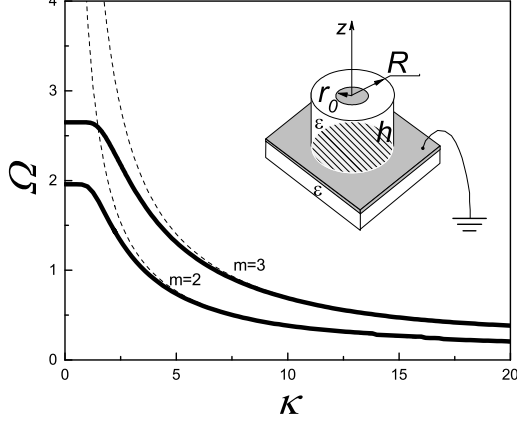


FIG. 1: Inset: the experimental setup. Main panel: the dimensionless frequency $\Omega = \omega/\omega_0(\varepsilon)$ vs screening parameter $\kappa = \sqrt{R/2h}$ for lowest plasma modes with $\alpha_{02} = 3.831$ and $\alpha_{03} = 7.016$ respectively for totally covered atop 2DEG, i.e. when $r_0 = R$. Dashed curves represent the asymptotes $\Omega = \frac{\alpha_{0m}}{\kappa}$ for highly screened 2D gas.

behavior of the second term in Eq.(5). The condition of zero current at the disk center $\rho = 0$ is fulfilled identically since $I \sim \rho \frac{\partial U}{\partial \rho} |_{\rho=0} = 0$. The outer boundary condition on the circumference of the disk requires a detailed analysis. Recent studies^{26,27} clearly demonstrate an anomalous Goos-Hänchen phase shift of incident and reflected plasma waves caused by presence of near-field evanescent waves at the sharp edge of 2D crystal. Although this effect is indeed fundamental, the present scheme of a grounded 2D system²¹⁻²³ relevant in our case does not meet the criterion of a sharp edge of 2D crystal. Therefore, we will assume a simple case of zero peripheral current $I(R) \sim J'_0(R/\lambda) = 0$. The later gives the dispersion equation for plasmon excitations

$$\omega \sqrt{LCR} = \alpha_{0m}. \quad (6)$$

Similar to Ref.¹² we will use the notation α_{0m} for m th zero of the function $J'_0(x)$. Using Eq.(3) we re-write Eq.(6) as it follows

$$\omega = v_p \frac{\alpha_{0m}}{R} \cdot \left[\frac{1 - e^{-2hq}}{2hq} \right]^{1/2}, \quad (7)$$

where $v_p = \sqrt{\frac{4\pi e^2 nh}{m^* \varepsilon}}$ is plasma wave velocity.

For strong screening case $qh \ll 1$ we obtain the relationship

$$\omega = v_p \frac{\alpha_{0m}}{R}, \quad (8)$$

which is exactly the linear dispersion law^{2,12} if one defines wave vector

$$q = \frac{\alpha_{0m}}{R} \quad (9)$$

for present case of axisymmetric plasmon excitations.

In the opposite ungated case $qh \gg 1$ Eq.(7) provides familiar long-wavelength dispersion law¹

$$\omega = \sqrt{\frac{2\pi e^2 n}{m^* \varepsilon}} q \quad (10)$$

with the wave vector specified by Eq.(9) as well.

Let's do visualization of the transition from ungated to screened 2D system by fixing the disk radius and, then varying the slab height. It is convenient to introduce the screening parameter $\kappa = \sqrt{R/2h}$ and reference value of frequency

$$\omega_0(\varepsilon) = \sqrt{\frac{2\pi e^2 n}{m^* \varepsilon R}}. \quad (11)$$

Using Eq.(7) we plot in Fig.1 the dimensionless frequency $\Omega = \omega/\omega_0(\varepsilon)$ vs κ for lowest axisymmetric modes $m = 2, 3$. For highly screening case $\kappa \gg 1$ one obtains $\Omega = \frac{\alpha_{0m}}{\kappa}$ being a simple replica of Eq.(8). For ungated 2D gas $\kappa \ll 1$ we recover the result specified by Eq.(10) as $\Omega = \sqrt{\alpha_{0m}}$. The change in axisymmetric mode behavior occurs at $\kappa \sim \sqrt{\alpha_{0m}}$ which was not clearly indicated in longstanding classical study¹².

The second part of the present paper concerns more interesting case of partially gated 2D electron system shown in Fig.1, inset. Let the height of the plate h be fixed. Obviously, the extension of the central gate spot would result in a transition from ungated to fully gated 2D gas. We now search the spectra of axisymmetric excitations by varying the central gate radius $0 \leq r_0 \leq R$.

For gated disk(index "1") and ungated ring(index "2") the in-plane potential can be written by Eq.(5) taking into account the respective inductances and capacitances specified by Eq.(3).

$$U_1 = A_1 J_0(\rho_1) \quad (12)$$

$$U_2 = A_2 J_0(\rho_2) + B_2 Y_0(\rho_2) \quad (13)$$

$$U_1 = U_2 |_{r=r_0}, U'_1 = U'_2 |_{r=r_0}, U'_2 |_{r=R} = 0, \quad (14)$$

where the dimensionless variables $\rho_{1,2} = r/\lambda_{1,2}$ are different for gated disk and ungated ring since $\lambda_{1,2} = \frac{1}{\omega \sqrt{LC_{1,2}}}$. The

actual experiments data²¹⁻²³ match the requirement $qh \ll 1$ valid for both the gated disk and the ungated ring. Using Eq.(3) we find $C_1 = \varepsilon r/2h$ for the gated part. However, for ungated part one needs to account the permittivity of the air above the ring. For actual $qh \ll 1$ case the rigorous analysis²⁸ provides $C_2 = \tilde{\varepsilon} qr$, where $\tilde{\varepsilon} = (1 + \varepsilon)/2$ denotes the effective dielectric permittivity.

Equations(12),(13) have to be solved under certain boundary conditions. As before, we will assume a zero current at both the circumference and the center of 2D disk. The boundary conditions for interface between the gated and ungated parts are of special interest. Recall that the conventional LC-approach¹⁹ concerns a two-dimensional stripe along, for example, x-direction. Theory states²⁹ that both the in-plane voltage U and the average complex power P carried by plasmon wave are constants across the interface between gated-to-ungated parts. The power is, in turn, determined by the longitudinal component of the Poynting vector $S_x = c[\vec{E}\vec{H}]_x/4\pi$

averaged over the oscillation period. Here, \vec{H} denotes the transverse magnetic field induced by plasmon propagating along two-dimensional stripe. Obviously, two-dimensional disk is not a case. Indeed, for arbitrary radial current the magnetic field is zero. Hence, the boundary conditions at the interface between the gated and ungated parts must be different compare to stripe case. It is natural and physically sensible to assume the potential and current as constants at the interface which is depicted by Eq.(14). Using the set of Eqs.(12,13,14) we obtain the transcendental dispersion equation

$$J_0(\Omega\Lambda\kappa\nu)(J_1(\Omega^2\nu)Y_1(\Omega^2) - J_1(\Omega^2)Y_1(\Omega^2\nu)) + \quad (15)$$

$$\frac{k\Lambda}{\Omega}J_1(\Omega\Lambda\kappa\nu)[J_1(\Omega^2)Y_0(\Omega^2\nu) - J_0(\Omega^2\nu)Y_1(\Omega^2)] = 0,$$

where $\Omega = \omega/\omega_0(\tilde{\varepsilon})$ is the dimensionless frequency, $\Lambda = \sqrt{\varepsilon/\tilde{\varepsilon}}$ is the auxiliary coefficient. Eq.(15) can be minimized as it follows

$$D_U \cdot \Re_I + \frac{k\Lambda}{\Omega}D_I \cdot \Re_U = 0. \quad (16)$$

Eq.(16) allows one to obtain the plasmon frequency Ω vs dimensionless ratio $\nu = r_0/R$ at certain value of parameters κ, Λ . Here, we use the notations $D_I = J_1(\Omega\Lambda\kappa\nu)$ and $D_U = J_0(\Omega\Lambda\kappa\nu)$ for gated disk(D) part. The solutions $D_{I(U)} = 0$ correspond to zero current at the disk center and, then the zero current(voltage) respectively at the disk circumference. The remaining multipliers, namely $\Re_I = J_1(\Omega^2\nu)Y_1(\Omega^2) - J_1(\Omega^2)Y_1(\Omega^2\nu)$ and $\Re_U = J_1(\Omega^2)Y_0(\Omega^2\nu) - J_0(\Omega^2\nu)Y_1(\Omega^2)$ correspond to ungated ring(\Re) part seen in Fig.1, inset. The transcendental equations $\Re_{I(U)} = 0$ define the solution of Bessel Eq.(4) for zero current(voltage) respectively at the inner boarder and, then the absence of the current at the outer circumference of the ring.

For real systems²² the typical disk size $R = 0.25\text{mm}$ is much grater than the gate to 2D gas separation is $h = 370\text{nm}$, hence we find $\kappa = 18 \gg 1$. Then, for GaAs/AlGaAs 2D system $\varepsilon = 12.8$ one obtains $\Lambda = 1.36$. Assuming that $\Omega \sim 1$ we conclude that second summand in Eq.(16) prevails. Therefore, the zeroth of transcendental equation $D_I = 0$ basically defines the solution of Eq.(16). The later condition corresponds to axisymmetric plasmon localized in a gated part. The respective frequencies are given by asymptotes $\Omega = \frac{\alpha_{0m}}{\kappa\Lambda\nu}$ shown by dotted lines in Fig.2. However, this simple scenario fails when the multipliers from first(second) summand in Eq.(16) vanish simultaneously $D_U, \Re_U = 0$ providing the dispersion Eq.(16) becomes fulfilled as well. The solutions of equations $D_U = 0$ and $\Re_U = 0$ are shown in Fig.2 by thin and dashed lines respectively. The condition $D_U, \Re_U = 0$ exactly defines the transition between neighboring axisymmetric modes. To support our reasoning we plot schematically in Fig.2, inset A the spatial distribution of the current in a disk for initial $m = 3$ and, then final $m = 2$ neighboring plasma modes. Actually, the transition $3 \rightarrow 2$ depicted as A in Fig.2 can be viewed as a plasma wave that loses half of the period.

For small gate sizes when the most place atop the slab is occupied by ungated ring, the lowest mode $m = 2$ undergo

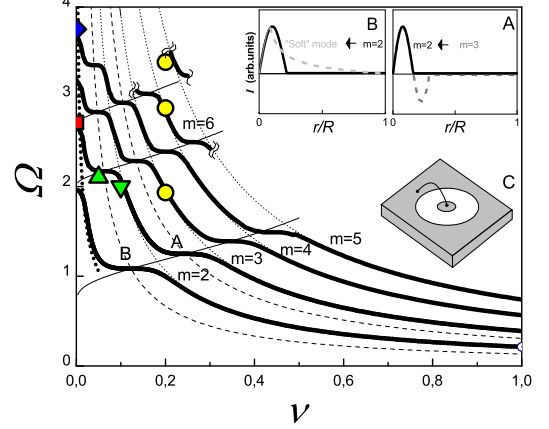


FIG. 2: The dimensionless frequency $\Omega = \omega/\omega_0(\tilde{\varepsilon})$ vs ratio $\nu = r_0/R$ for lowest $m = 2..5$ and, partially $m = 6, 8$ plasma modes plotted for fixed $\kappa = 18, \Lambda = 1.36$. Arrows depict the frequency $\Omega = \sqrt{\alpha_{0m}}$, $m=2..5$ for totally ungated 2DEG. Dotted lines represent the asymptotes $\Omega = \frac{\alpha_{0m}}{\kappa\Lambda\nu}$ expected for plasmon localized in the gated part. Dashed(solid thin) lines depict $D_U = 0$ and $\Re_U = 0$ solutions respectively. Bold dotted line specifies the "soft" mode asymptote $\Omega = \frac{1}{\sqrt{\kappa\Lambda\nu}}$. The experimental data for ungated ($\square^{22}, \diamond^{23}$) and partially gated ($\triangle, \nabla, \circ^{21}$) 2D systems is denoted in Table 1. Inset A(B): Radial distribution(schematically) of the current density for and intermode transition A and B respectively shown in the main panel. Inset C: Feedback 2D plasmon resonator(under Ref.³⁰).

further transformation. The point of interest B in Fig.2 is still defined by condition $D_U, \Re_U = 0$. However, in the present case the plasmon mode $m = 2$ is first confined within ultra-narrow gated part and, then is modified entirely by occupation of the ungated part as whole. Let us call further this mode as "soft" mode. In Fig.2 we represent schematically the current spatial distribution for initial $m = 2$ mode and, finally, the "soft" mode. We verify the dispersion relation for "soft" mode follows the asymptote $\Omega = \frac{1}{\sqrt{\kappa\Lambda\nu}}$ shown by bold dotted line in Fig.2. In actual fact, the appearance of the "soft" mode is a precursor of the conventional plasmon localized in completely ungated 2D gas, i.e. when $\Omega = \sqrt{\alpha_{0m}}$.

It is worthwhile to mention with respect to Fig.2 that upon change of the gate radius r_0 the plasmon frequency follows either $\omega \sim 1/r_0$ or $\omega \sim 1/\sqrt{R}$ dependencies regarding to the actual ν -range of interest. Evidently, this uncertainty may lead in misunderstanding regarding accurate identification of the plasmon modes. We argue that the present model would be useful for analyzing the axisymmetric plasmon excitations persisting in partially gated 2D disk feedback system³⁰ shown in Fig.2, inset.

Let us compare our results with experimental data for Al-GaAs/GaAs samples demonstrated²¹⁻²³ axisymmetric plasmon excitations. At first, we calculate the reference frequency $f_0 = \omega_0(\tilde{\varepsilon})/2\pi$ for each specimen presented in Table 1. To confirm validity of our quasistatic approach, we calculate the ratio of the long-wavelength plasma frequency to light fre-

TABLE I: Axisymmetric plasmon: theory vs experiment

Samp.	$n \cdot 10^{11}$ [cm ⁻²]	h [nm]	r_0 [mm]	R [mm]	f_0 [GHz]	A	f_{exp} [GHz]	Ω_{exp}	Ref.
N1	2.6	-	0	0.25	30.0	0.31	60.0	1.0	□ ²²
N2	1.0	370	0.05	1.0	9.3	0.38	14.4	1.6	△ ²¹
N3	1.0	370	0.05	0.50	13.2	0.27	19.4	1.5	▽ ²¹
N4	1.0	370	0.05	0.25	18.6	0.19	26.5	1.4	○ ²¹
N4	1.0	370	0.05	0.25	18.6	0.19	39.4	2.1	○ ²¹
N4	1.0	370	0.05	0.25	18.6	0.19	46.4	2.5	○ ²¹
N5	1.0	-	0	0.50	13.2	0.27	36.4	2.8	◇ ²³
N5	1.0	-	0	0.50	13.2	0.27	47.0	3.6	◇ ²³

quency with the same wave vector, $A = \omega_0(\tilde{\epsilon})\sqrt{\tilde{\epsilon}}R/c$, called retardation parameter¹¹. For all samples in Table 1 $A \ll 1$. We conclude that retardation effects are insignificant, therefore the use of non-retarded Poisson's equation is well justified.

Continuing the analysis of experimental data we calculate the dimensionless ratio $\Omega_{exp} = f_{exp}/f_0$ for each sample. The resulting data points are then added to the graph of the plasmon spectra in Fig.2. Remarkably, the experimental values match perfectly the certain modes of axisymmetric plasmon spectrum. For samples N1,2 the lowest observed plasmon

mode corresponds to $m = 2$, then the plasmon in sample N3 exhibits $m = 3$ mode. The sample N4 demonstrated a series of the plasmon modes $m = 4, 5, 6$. The ungated sample N5 exhibited the plasma mode for $m = 3, 5$. For samples N3-5, expected strong the fundamental axisymmetric mode $m = 2$ was not observed. Although this finding looks puzzling, the answer is unpretentious. Recall that for dark axisymmetric plasmon excitation the coupling with external electromagnetic radiation is much weaker²¹ compared to conventional plasmons with nonzero angular momentum $l \neq 0$. Evidently, the dark modes would be hidden out by conventional ones. Indeed, the conventional $l = 1$ modes observed²² at frequencies 18GHz and 13GHz cover the spectral range of axisymmetric fundamental modes expected at 14.2GHz and 13.7GHz for samples N4 and N3 respectively. Finally, for sample N5 one expects the fundamental dark mode at 25.6GHz which close to²³ with conventional mode $l = 1$ at 19GHz.

In conclusion, we investigated the transition from ungated to gated two-dimensional system of disk geometry by means of central spot gate expansion. The discontinuity of gated to ungated part provides the interchange between the neighboring axisymmetric modes. The experimental data for different sample sizes, carrier densities is found to agree well with theory predictions. Our study allows to classify the observed dark axisymmetric modes and, moreover, pave a way to feedback plasmon resonator³⁰ study.

- ¹ F. Stern, Polarizability of a Two-Dimensional Electron Gas, Phys. Rev. Lett. 18 (1967) 546, <https://doi.org/10.1103/PhysRevLett.18.546>.
- ² A.V. Chaplik, Possible Crystallization of Charge Carriers in Low-Density Inversion Layers, Zh. Eksp. Teor. Fiz. 62 (1972) 746 [Sov. Phys. JETP 35 (1972) 395].
- ³ C.C. Grimes and G. Adams, Observation of Two-Dimensional Plasmons and Electron-Ripplon Scattering in a Sheet of Electrons on Liquid Helium, Phys. Rev. Lett. 36 (1976) 145, <https://doi.org/10.1103/PhysRevLett.36.145>.
- ⁴ S.J. Allen, D.C. Tsui and R.A. Logan, Observation of the Two-Dimensional Plasmon in Silicon Inversion Layers, Phys. Rev. Lett. 38 (1977) 98, <https://doi.org/10.1103/PhysRevLett.38.980>.
- ⁵ T.N. Theis, J.P. Kotthaus and P.J. Stiles, Wavevector dependence of the two-dimensional plasmon dispersion relationship in the (100) silicon inversion layer, Solid State Commun. 26 (1978) 603, [https://doi.org/10.1016/0038-1098\(78\)90773-1](https://doi.org/10.1016/0038-1098(78)90773-1).
- ⁶ D.Heitmann, J.P. Kotthaus, and E.G. Mohr, Plasmon dispersion and intersubband resonance at high wavevectors in Si(100) inversion layers, Solid State Commun. 44 (1982) 715, [https://doi.org/10.1016/0038-1098\(82\)90590-7](https://doi.org/10.1016/0038-1098(82)90590-7).
- ⁷ D.C. Tsui, E. Gornik, and R.A. Logan, Far infrared emission from plasma oscillations of Si inversion layers, Solid State Commun. 35 (1980) 875, [https://doi.org/10.1016/0038-1098\(80\)91043-1](https://doi.org/10.1016/0038-1098(80)91043-1).
- ⁸ K.W. Chiu and J.J.Quinn, Plasma oscillations of a two-dimensional electron gas in a strong magnetic field, Phys. Rev. B 9 (1974) 4724, <https://doi.org/10.1103/PhysRevB.9.4724>.
- ⁹ M. Nakayama, Theory of Surface Waves Coupled to Surface Carriers, J.Phys. Soc. Jpn. 36 (1974) 393, <https://doi.org/10.1143/JPSJ.36.393>
- ¹⁰ V.A. Volkov and S.A. Mikhailov, Edge magnetoplasmons: Low

- frequency weakly damped excitations in inhomogeneous two-dimensional electron systems, Sov. Phys. JETP 67 (1988) 1639.
- ¹¹ I.V. Kukushkin, J.H. Smet, S.A. Mikhailov, D.V. Kulakovskii, K.von Klitzing and W. Wegscheider, Observation of Retardation Effects in the Spectrum of Two-Dimensional Plasmons, Phys. Rev. Lett. 90 (2003) 156801, <https://doi.org/10.1103/PhysRevLett.90.156801>.
- ¹² A.L. Fetter, Magnetoplasmons in a two-dimensional electron fluid: Disk geometry, Phys. Rev. B 33 (1986) 5221, <https://doi.org/10.1103/PhysRevB.33.5221>.
- ¹³ Yu.A. Kosevich, A.M. Kosevich, J.C. Granada, Magnetoplasma oscillations of a two-dimensional electron layer in a bounded system, Phys. Lett. A 127 (1988) 52, [https://doi.org/10.1016/0375-9601\(88\)90964-4](https://doi.org/10.1016/0375-9601(88)90964-4).
- ¹⁴ A.A. Zabolotnykh and V.A. Volkov, Magnetoplasmon-polaritons in a two-dimensional electron system with the back gate, Pis'ma Zh. Eksp. Teor. Fiz. 115 (2022) 163 [JETP Lett. 115 (2022) 141], <https://doi.org/10.1134/S0021364022030110>.
- ¹⁵ V.I. Falko and D.E.Khmel'nitskii, What if a film conductivity exceeds the speed of light? Zh. Eksp. Teor. Fiz. 95 (1989) 1988 [Sov. Phys. JETP 68 (1989) 1150].
- ¹⁶ M.V. Cheremisin, Magnetoplasmon spectrum for realistic off-plane structure of dissipative 2D system, Solid State Commun. 268 (2017) 7, <https://doi.org/10.1016/j.ssc.2017.09.013>.
- ¹⁷ P.J. Burke, I.B. Spielman, and J.P. Eisenstein, High frequency conductivity of the high-mobility twodimensional electron gas, Appl. Phys. Lett. 76 (2000) 745, <https://doi.org/10.1063/1.125881>.
- ¹⁸ F. Rana, Graphene Terahertz Plasmon Oscillators, IEEE Trans. Nanotech. 7 (2008) 91, <https://doi.org/10.1109/TNANO.2007.910334>.

- ¹⁹ G.C. Dyer, G.R. Aizin, Transmission line theory of collective plasma excitations in periodic two-dimensional electron systems: Finite plasmonic crystals and Tamm states, *Phys. Rev. B* 86 (2012) 235316, <https://doi.org/10.1103/PhysRevB.86.235316>.
- ²⁰ G.C. Dyer, G.R. Aizin, S.J. Allen, A.D. Grine, D. Bethke, J. L. Reno, and E.A. Shaner, Induced transparency by coupling of Tamm and defect states in tunable terahertz plasmonic crystals, *Nature Photon.* 7 (2013) 925, <https://doi.org/10.1038/nphoton.2013.252>.
- ²¹ V.M. Muravev, I.V. Andreev, V.N. Belyanin, S.I. Gubarev, and I.V. Kukushkin, Observation of axisymmetric dark plasma excitations in a two-dimensional electron system, *Phys. Rev. B* 96 (2017) 045421, <https://doi.org/10.1103/PhysRevB.96.045421>.
- ²² A.A. Zagitova, V.M. Muravev, P.A. Gusikhin, A.A. Fortunatov, I.V. Kukushkin, Observation of "dark" axisymmetric plasma modes in a single disk of two-dimensional electrons, *Pis'ma Zh. Eksp. Teor. Fiz.* 108 (2018) 478 [*JETP Lett.* 108 (2018) 446], <https://doi.org/10.1134/S0021364018190141>.
- ²³ A.M. Zarezin, D. Mylnikov, A.S. Petrov, D. Svintsov, P.A. Gusikhin, I.V. Kukushkin, V.M. Muravev, Plasmons in a Square of Two-Dimensional Electrons, *Phys. Rev. B* 107 (2023) 075414, <https://doi.org/10.1103/PhysRevB.107.075414>.
- ²⁴ I.V. Zagorodnev, D.A. Rodionov and A.A. Zabolotnykh, Effect of retardation on the frequency and linewidth of plasma resonances in a two-dimensional disk of electron gas, *Phys. Rev. B* 103 (2021) 195431, <https://doi.org/10.1103/PhysRevB.103.195431>.
- ²⁵ D.A. Rodionov, I.V. Zagorodnev, A.A. Zabolotnykh, and V.A. Volkov, Axisymmetric plasma mode in disk with two-dimensional electron gas, *J. Phys.: Conf. Ser.* 1686 (2020) 012052, <https://doi.org/10.1088/1742-6596/1686/1/012052>.
- ²⁶ A.Y. Nikitin, T. Low, L. Martin-Moreno, Anomalous reflection phase of graphene plasmons and its influence on resonators, *Phys. Rev. B* 90 (2014) 041407(R), <https://doi.org/10.1103/PhysRevB.90.041407>.
- ²⁷ Ji-Hun Kang, Sheng Wang, Zhiwen Shi, Wenyu Zhao, Eli Yablonovitch, and Feng Wang, Goos-Hänchen shift and even-odd peak oscillations in edge reflections of surface polaritons in atomically thin crystals, *Nano Lett.* 17 (2017) 1768, <https://doi.org/10.1021/acs.nanolett.6b05077>.
- ²⁸ S. Siaber, S. Zonetti, J.E. Cunningham and O. Sydoruk, Terahertz Plasmon Resonances in Two-Dimensional Electron Systems: Modeling Approaches, *Phys. Rev. Appl.* 11 (2019) 064067, <https://doi.org/10.1103/PhysRevApplied.11.064067>.
- ²⁹ J.R. Brews, Characteristic Impedance of Microstrip Lines, *IEEE Trans. Microw. Theor. Tech.* 35 (1987) 30, <https://doi.org/10.1109/TMTT.1987.1133591>.
- ³⁰ V.M. Muravev, P.A. Gusikhin, A.M. Zarezin, A.A. Zabolotnykh, V.A. Volkov and I. V. Kukushkin, Physical origin of relativistic plasmons in a two-dimensional electron system, *Phys. Rev. B* 102 (2020) 081301(R), <https://doi.org/10.1103/PhysRevB.102.081301>.